

Supplemental data

Supplemental methods

Expression Plasmids and siRNA. The full-length human WHSC1 cDNA was cloned into pMSCV-puro/neo (Clontech), pcDNA5 (Flag tag) (Invitrogen), pDEST20 (Invitrogen) and pcDNA3.1 (Myc tag) (Invitrogen) to generate WHSC1 expression plasmids. A gRNA expression plasmid was generated by cloning annealed gRNA oligonucleotides into the pX330. A double strand of DNA of 1600 bp in size was designed to serve as a template for HDR following the Cas9 induced double strand break. The template was designed with a dinucleotide polymorphism which when incorporated into the genome would result in an alternate codon encoding alanine acid (A) instead of the native serine (S). The shRNA, gRNA and siRNA sequences are listed in Supplemental Table 5.

Cell culture and reagents. PC3, LNCaP and DU145 cells were obtained from ATCC and cultured in DMEM or RPMI supplemented with 10% fetal bovine serum. RWPE-1 cells (ATCC) were cultured with Keratinocyte Serum Free Medium (K-SFM) (Invitrogen) with bovine pituitary extract and human recombinant epidermal growth factor (EGF). Cells were transfected with siRNA duplexes (60-100 nM) by using Lipofectamine (Invitrogen) or Dharmacon Transfection (Dharmacon) reagents according to manufacturer's instructions. To establish individual stable cells, retrovirus/lentivirus was used. Cell proliferation assay was performed using CellTiter 96® Non-Radioactive Cell Proliferation Assay (MTT) kit (Promega) according to the manufacturer's instructions. Standard 24-well Boyden invasion chambers (BD Biosciences) were used to assess cell migration abilities following the manufacturer's suggestions. For soft-agar colony formation assay, cells were suspended in RPMI1640 containing 0.35% low-melting agar (Invitrogen) and 10% FBS and seeded onto a coating of 0.7% low-melting agar in RPMI1640 containing 10% FBS. Plates were incubated at 37 °C and 5% CO₂ and colonies were scored 3 weeks after preparation. Colonies larger than 0.1 mm diameter were scored as positive. Results were calculated based on 3 independent experiments and statistical significance was determined by One-way ANOVA (Tukey's multiple comparisons test).

RNA isolation and real-time PCR. Total RNA was extracted using TRIzol followed by RNeasy Mini kit (Qiagen) cleanup and RQ1 RNase-free DNase Set treatment (Promega) according to the manufacturer's instructions. First strand cDNA was synthesized using Superscript II (Invitrogen) and 2 µg of total RNA was used in each cDNA synthesis reaction. Syber green Universal Master Mix reagents (Roche) and primer mixtures (Supplemental Table 6) were used for the real-time PCR. Standard curves were generated by serial dilution of a preparation of total RNA, and all mRNA quantities were normalized against β-actin RNA. Student's t-test or One-way ANOVA (Tukey's multiple comparisons test) was used to statistical analysis of qRT-PCR results and p value less than 0.05 was considered significant.

Baculovirus Expression of Full-Length WT and S172 mutated WHSC1 protein. Generation and purification of recombinant full-length WHSC1, WHSC1-S172A and WHSC1-172D were performed following the manufacturers' manuals (Invitrogen). In brief, pDEST20-WHSC1 was utilized to transform DH10Bac E. coli to obtain shuttle bacmid. Sf9 cells were transfected with bacmid DNA to produce baculovirus particles and the virus titer was amplified through multiple rounds of transduction. Sf9 cells were transduced with virus stock and cells were harvested 3 days after transduction. The His-tagged recombinant proteins were purified using HisTrap™ FF crude columns (GE Healthcare), and the quality of the purified proteins was monitored by SDS-PAGE followed by Coomassie staining.

Assay with MEFs. MEFs were isolated from embryonic day (E) 12.5 embryos and cultured in DMEM medium supplemented with 10% FBS, penicillin/streptomycin, and 2 mM L-glutamine using standard techniques. Ad-GFP and Ad-Cre virus were used to infect the cells at MOI = 5.

Immunocytochemistry, immunoprecipitation and immunoblotting. For immunocytochemistry, cells were fixed with 4% formalin for 15 minutes, permeated with 0.1% Triton X-100 for 10 minutes, and stained with 200 nM rhodamine phalloidin (Invitrogen, R415) for 30 minutes. phospho-FAK (Invitrogen, 44-626G), P34arc (Millipore, 07-227) or phospho-Paxllin (Cell Signaling Technology, 2541) staining was performed as described previously. Stained cells

were then imaged with a laser confocal microscope. 6 random fields of view per sample were assessed with ZEN 2 software. For immunoprecipitation assays, cells were lysed with HEPES lysis buffer (20 mM HEPES, pH 7.2, 50 mM NaCl, 0.5% NP-40, 1 mM NaF and 1 mM dithiothreitol) supplemented with protease-inhibitor cocktail (Roche). Immunoprecipitations were performed using the indicated primary antibody and protein A/G agarose beads (Roche) at 4 °C. The immunocomplexes were then washed with HEPES lysis buffer four times. Both lysates and immunoprecipitates were examined using the indicated primary antibodies and the related secondary antibody followed by detection with the chemiluminescence substrate (Millipore).

Chromatin-immunoprecipitation assays. The ChIP assays were performed using Magnetic ChIP kit (Millipore). The procedure was as described in the kit provided by the manufacturer. Briefly, PC3 cells were fixed by 1% formaldehyde, fragmented by a combination of MNase and sonication. WHSC1 (abcam, ab75359), H3K27me3 (cell signaling, 9733), H3K36me2 (abcam, ab9049) and H3K9ac (cell signaling, 9649) antibody were then used for immunoprecipitation. After washing and reverse-crosslinking, the precipitated DNA was amplified by primers and quantified by the Step One Plus real-time-PCR machine. Primer sequences can be found in the Supplemental Table 6.

In vitro and in vivo ubiquitination assay. The procedure for in vitro ubiquitination assay was conducted according the manufacturer's instructions. Briefly, to purify the substrate, His tagged-WHSC1, WHSC1-S172A and WHSC1-S172D were expressed by baculovirus-insect cell system. To purify the endogenous CUL4B ligases, CUL4B immunocomplexes were immunoprecipitated from 293T cells transfected with Flag-CUL4B plasmids using Flag M2 beads (Sigma), and then eluted by incubating with a molar excess of Flag peptide. For the in vitro WHSC1 ubiquitination, the CUL4B immunocomplex was mixed with His-tagged wild-type or WHSC1 mutated substrate, and this mixture was added to a ubiquitin ligation reaction (Enzo Life Sciences). The reactions were incubated at 37 °C for 60 min, and the samples were submitted to immunoblotting with the anti-WHSC1 or Ub antibody to examine ubiquitin ladder formation. In vivo ubiquitination assays was performed in 293T cells

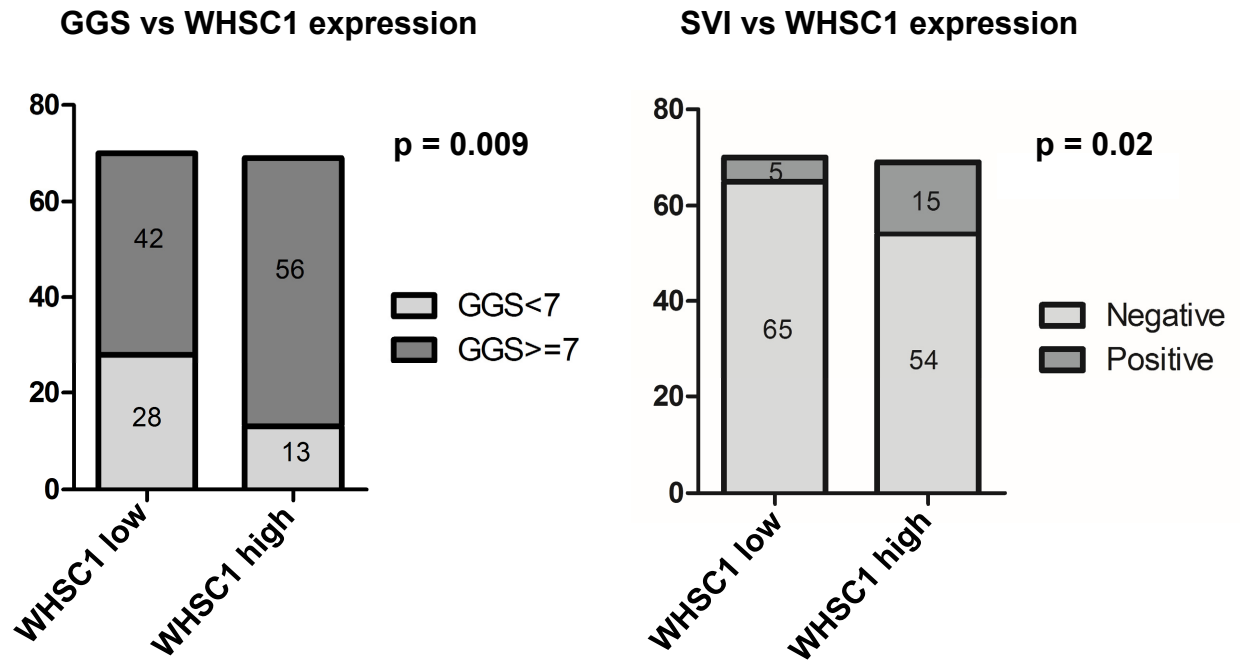
transfected with Flag-WHSC1, Flag-WHSC1 together with HA-Ub or endogenous parent and WHSC1-S172A mutant PC3 cells, which pre-treated with MG132 for 8 hours. Immunoprecipitations were performed using the indicated Flag or WHSC1 antibody and protein A/G agarose beads (Roche) at 4 °C and then subjected to Western blotting with antibodies specific for Ub (Cell signaling, 3933).

In Vitro Kinase Assay. AKT1 was purchased from Active motif. Briefly, 1 µg of indicated His tagged proteins were incubated with purified active AKT1 in the presence of 5 µCi [γ -³²P] ATP and 200 µM cold ATP in the reaction buffer for 15–30 min. The reaction was stopped by the addition of SDS-containing lysis buffer, resolved on SDS-PAGE, and detected by autoradiography.

In-gel digestion LC-ms/ms analysis, and protein identification. The protein bands were excised and in-gel digested. Then, liquid chromatography-mass spectrometry/mass spectrometry (LC-MS/MS) analyses of tryptic digests were performed on a Q-Exactive mass spectrometer (Thermo Fisher Scientific Inc.) interfaced with an EASY-nLC 1000 System (Thermo Fisher Scientific Inc.). LC-MS/MS data were analyzed by Mascot (v2.3, Matrix Science Ltd., London, UK). Peak lists were generated by Proteome Discoverer software (version 1.4) from Thermo Fisher. Precursor mass tolerance for Mascot analysis was set at ± 10 ppm, and fragment mass tolerance was set at ± 0.02 Da. The Mascot cutoff score was set to 20 ($p < 0.05$) to exclude the low score peptides.

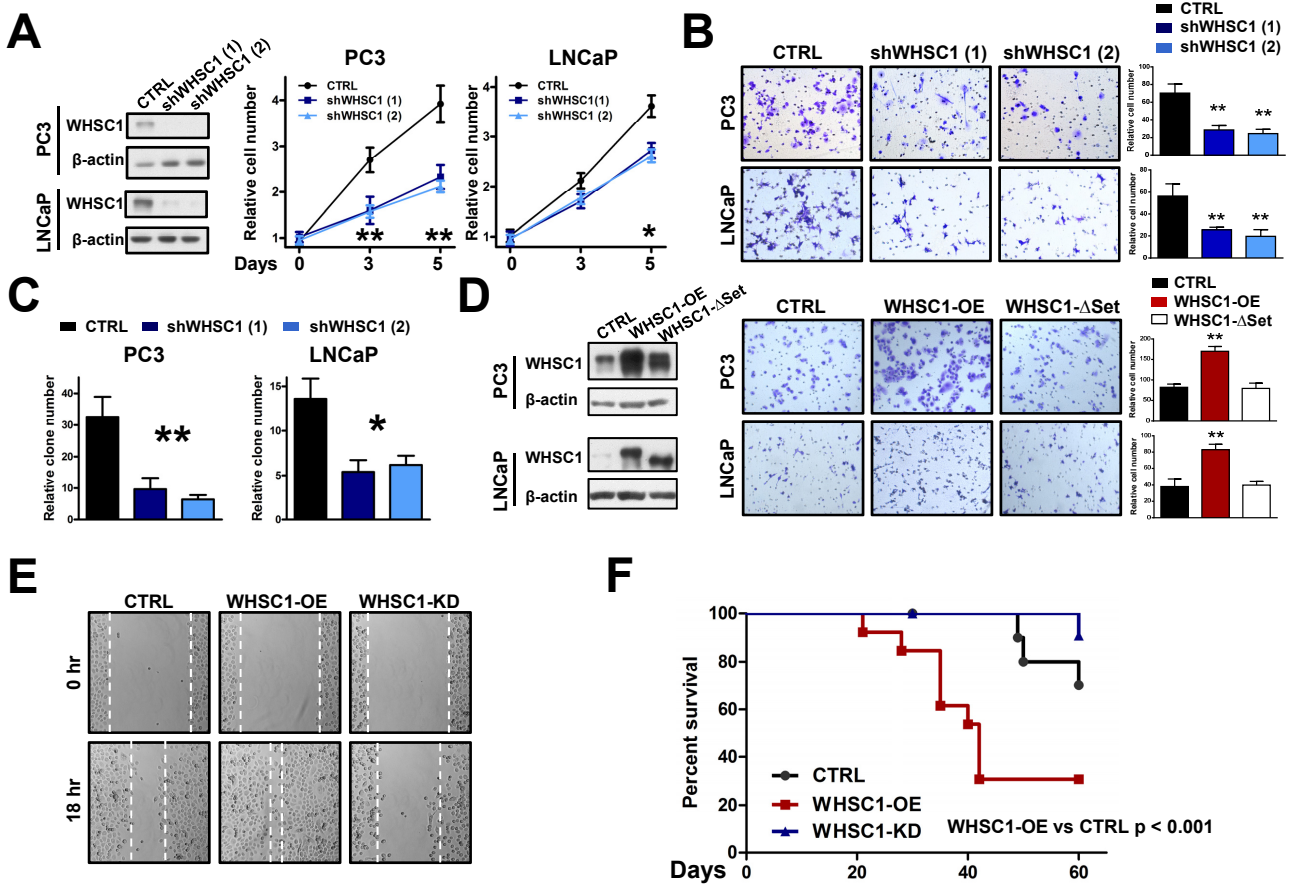
Supplemental Figure 1

GSE21032



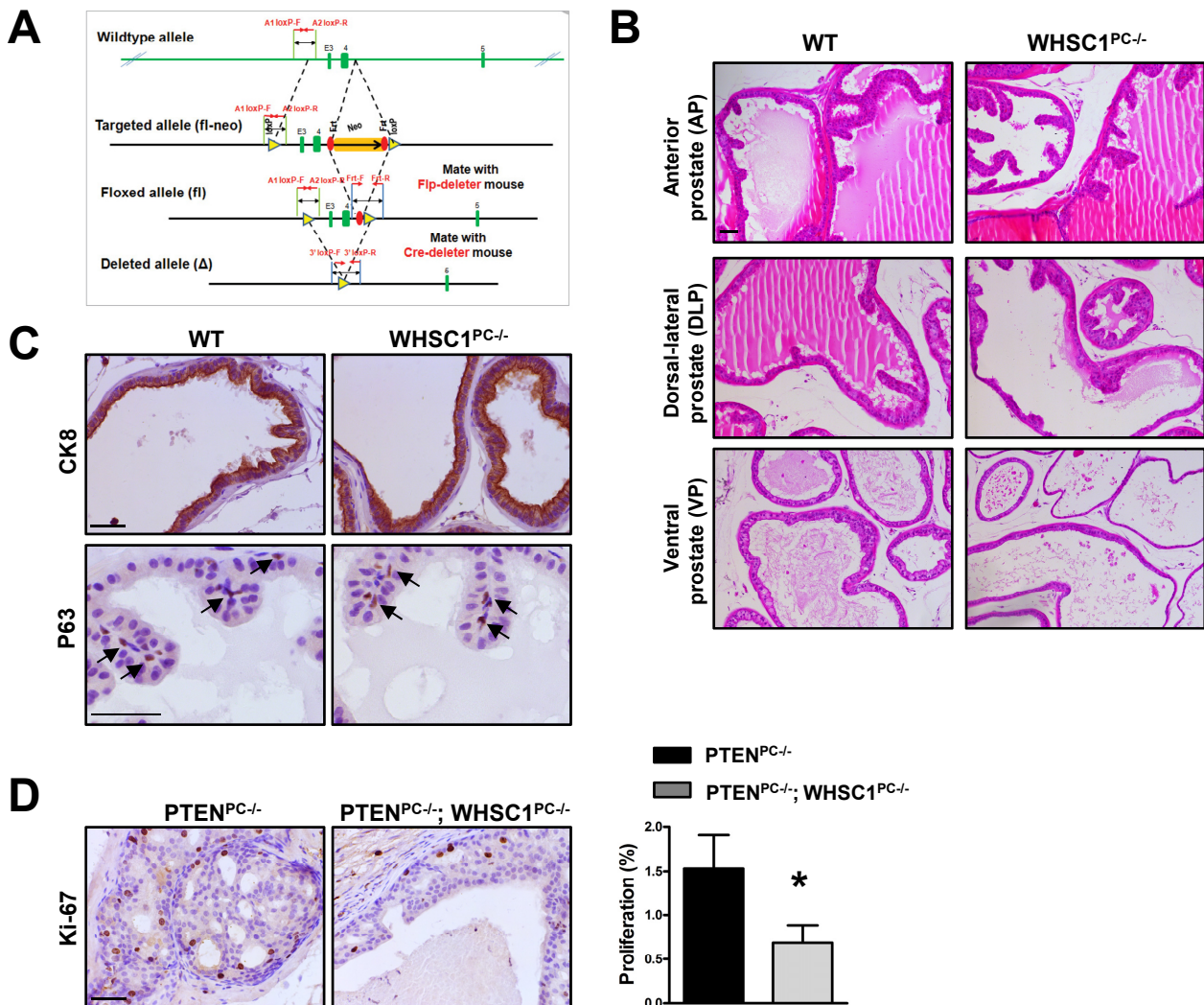
Supplemental Figure 1. Clinical associations of WHSC1 in PCa patients. The correlations between WHSC1 expression and Gleason score, seminal vesicle invasion are shown as stacked columns (using dataset GSE21032, n = 139). Fisher exact test is used to determine statistical significance.

Supplemental Figure 2



Supplemental Figure 2. WHSC1 is important for prostate tumorigenesis in PCa cells. (A) In vitro growth of control and WHSC1 depleted PC3 and LNCaP cells are measured by MTT analysis. WHSC1 knockdown efficiency is shown in left panel ($n = 3$). (B-C) In vitro transwell (B) and soft agar assays (C) examining migration abilities and the anchorage-independent growth of the parental and WHSC1 knockdown cells ($n = 3$). (D) In vitro transwell assay examining migration abilities of the parental and cells overexpressing wild-type WHSC1 or WHSC1- Δ Set, and quantitation results are shown in right panel ($n = 3$). (E) Wound healing assay of control, WHSC1 over-expression and WHSC1 knockdown PC3 cells (F) Animal survival of ex-vivo bone metastasis analysis of PC3 cells with WHSC1 depletion or over-expression in nude mice ($n = 9$ per group). Log-rank test is performed to compare animal survival. Results in A-E are presented as mean \pm SEM. *: $p < 0.05$, **: $P < 0.01$.

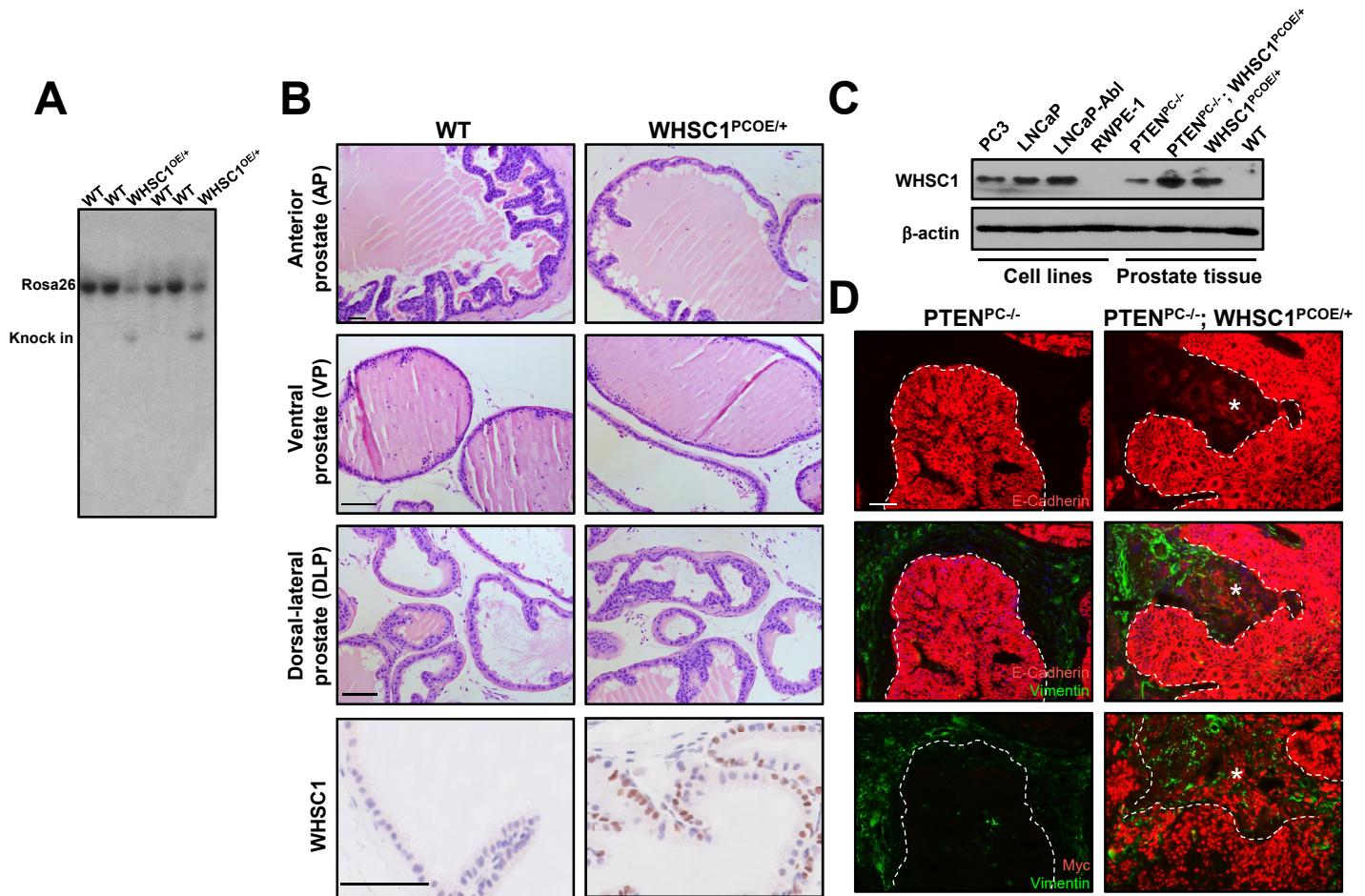
Supplemental Figure 3



Supplemental Figure 3. Inactivation of WHSC1 inhibits PTEN-deficient prostate tumor progression.

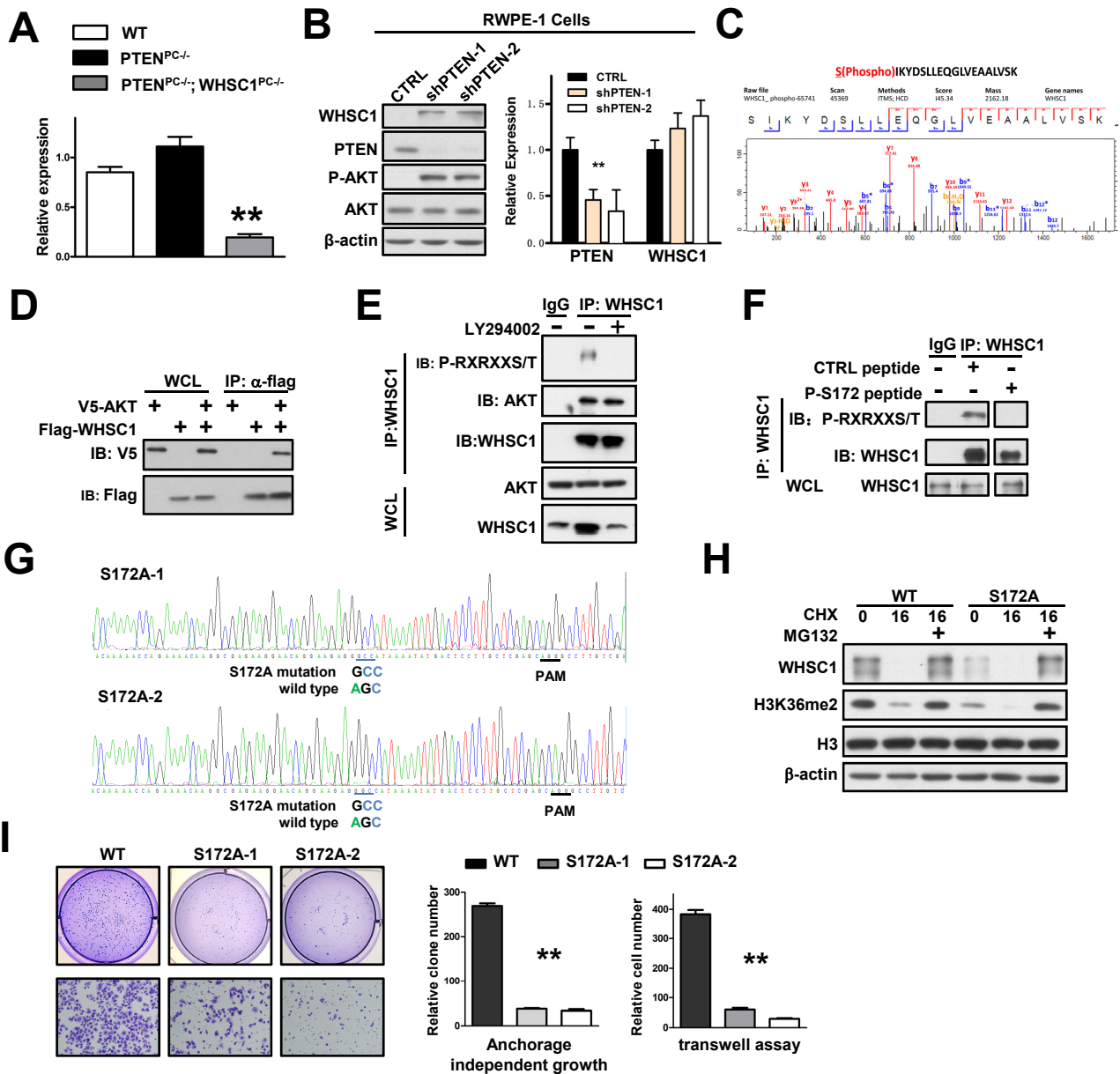
(A) Schematic generation of WHSC1 floxed alleles. (B) H&E staining sections of representative anterior prostate (AP), ventral prostate (VP), and dorsal-lateral prostate (DLP) at 4-month-old wild-type and WHSC1^{PC-/-} mice. (C) Immunohistochemical analysis of CK8 and p63 positive cells in prostate epithelium of wild-type and WHSC1^{PC-/-} mice. (D) Ki-67 staining of prostate sections from 4-month-old PTEN^{PC-/-} and PTEN^{PC-/-}; WHSC1^{PC-/-} mice, and semi-quantitative results are shown in the right panel. Results are presented as mean \pm SEM. *: $p < 0.05$. Scale bars: 50 μ m (B, C, D)

Supplemental Figure 4



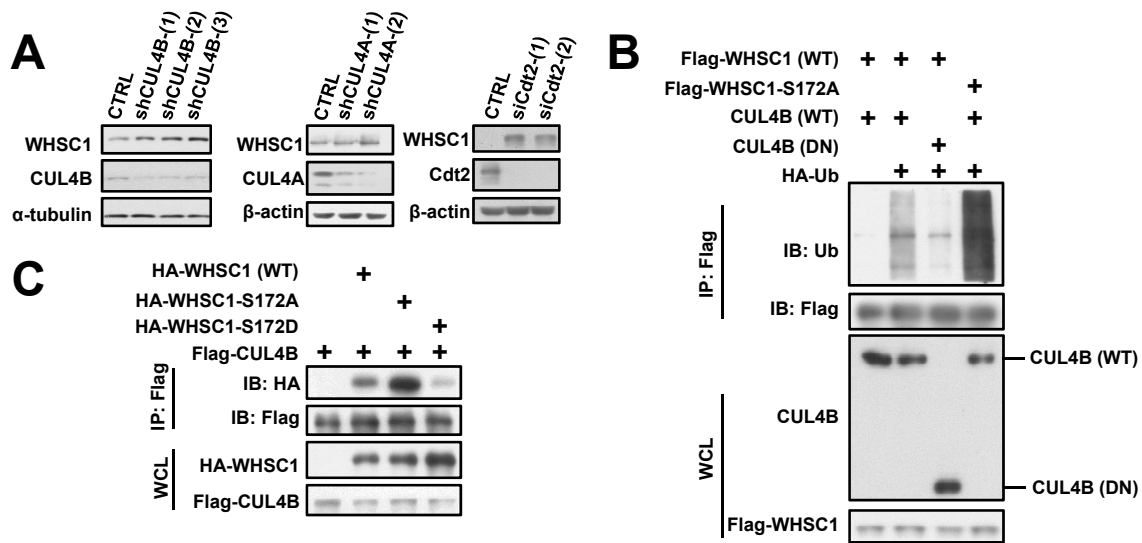
Supplemental Figure 4. Over-expression of WHSC1 potentiates the metastasis of PTEN null tumors. (A) Southern blotting analysis of genotyping of WHSC1^{OE/+} mice using mice tailing genomic DNA. (B) H&E staining sections of representative anterior prostate (AP), ventral prostate (VP), and dorsal-lateral prostate (DLP) at 8-month-old wild-type and WHSC1^{PCOE/+} mice and immunohistochemical analysis of WHSC1 expression in prostate epithelium from wild-type and WHSC1^{PCOE/+} mice (bottom). (C) Western blotting analysis of the indicated protein in normal (RWPE-1), prostate cancer cell lines (PC3, LNCaP and LNCaP-Abl) and in anterior prostate lysates of wild-type, PTEN^{PC-/-}, PTEN^{PC-/-}; WHSC1^{PCOE/+} and WHSC1^{PCOE/+} mice. (D) E-cadherin, Vimentin and Myc staining of prostate tumor sections of 4-month-old PTEN^{PC-/-} and PTEN^{PC-/-}; WHSC1^{PCOE/+} mice. Scale bars: 50 μ m (B and D)

Supplemental Figure 5



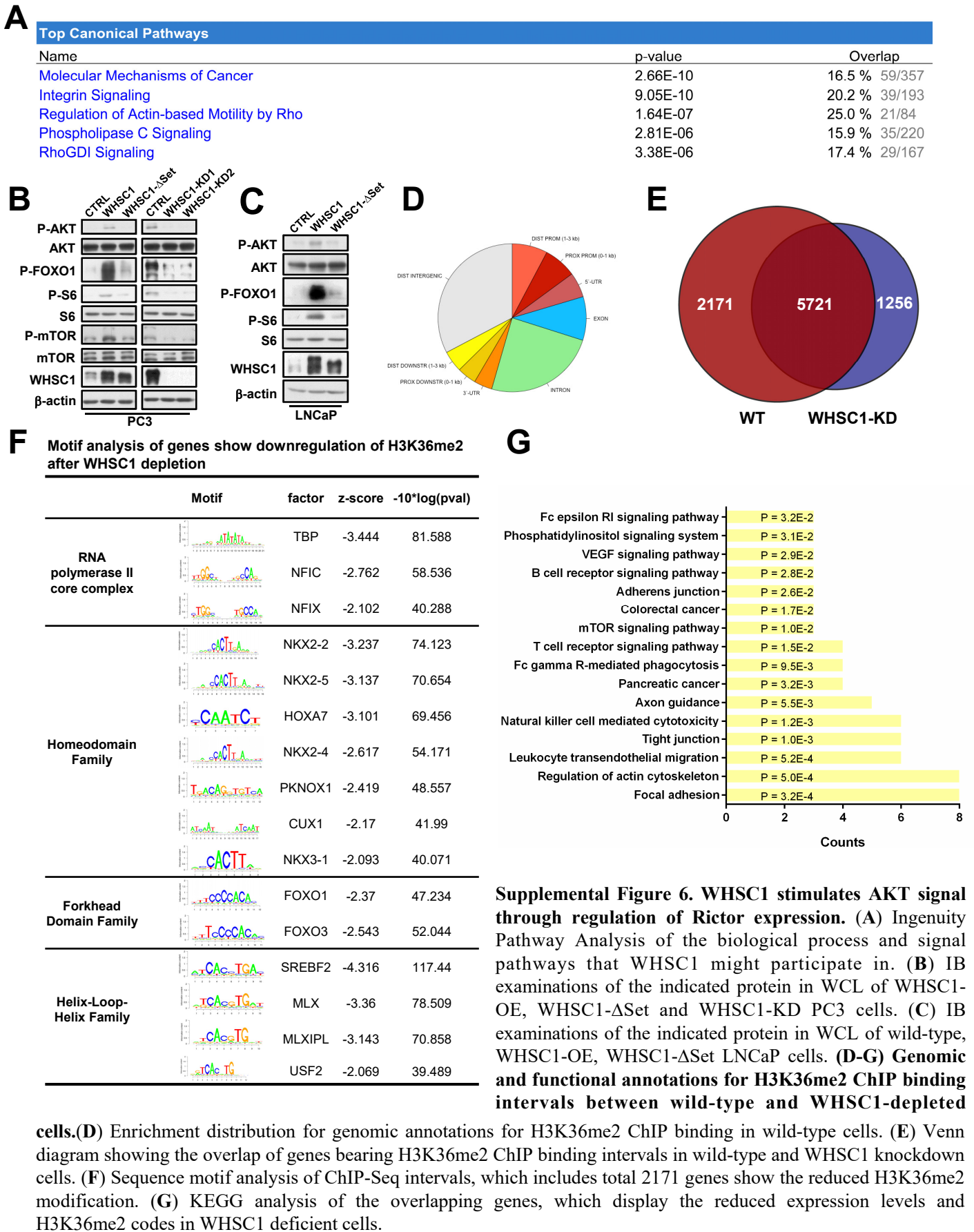
Supplemental Figure 5. AKT directly phosphorylates and stabilizes WHSC1 in PCa cells. (A) qRT-PCR analysis of WHSC1 transcripts in wild type, PTEN^{PC-/-} and PTEN^{PC-/-}; WHSC1^{PC-/-} mice. (B) Immunoblot analysis (IB) (left) and qRT-PCR analysis (right) of the indicated genes in RWPRE-1 cells depleting PTEN. Results are presented as mean \pm SEM. **: P < 0.01. (C) The MS/MS fragmentation spectrum showing distinct b- (N-terminal) and y- (C-terminal) series fragment ions for the WHSC1 peptide defining the pSer site in the degnon region. (D) IB analysis of WCL and immunoprecipitates (IP) derived from 293T cells transfected with V5-AKT and Flag-WHSC1. (E) IB analysis of WCL and IP derived from PC3 cells which were treated with 30 μ M LY294002 for 8 hours before harvesting. (F) The phospho-specificity of the antibody is demonstrated by peptide competition using phospho-peptides in Serine 172 site or a non-phosphorylated peptide as indicated. (G) Sequencing validations of CRISPR WHSC1-S172A knock-in allele in PC3 cells. (H) Wild-type or S172A mutated cells were treated with 100 μ g/ml cycloheximide (CHX), and IB analysis of WCL harvested at indicated time points. (I) Representative images of anchorage independent growth (upper) or transwell assays in control and S172A PC3 cells, and quantitation results are shown in right panel (n = 3).

Supplemental Figure 6

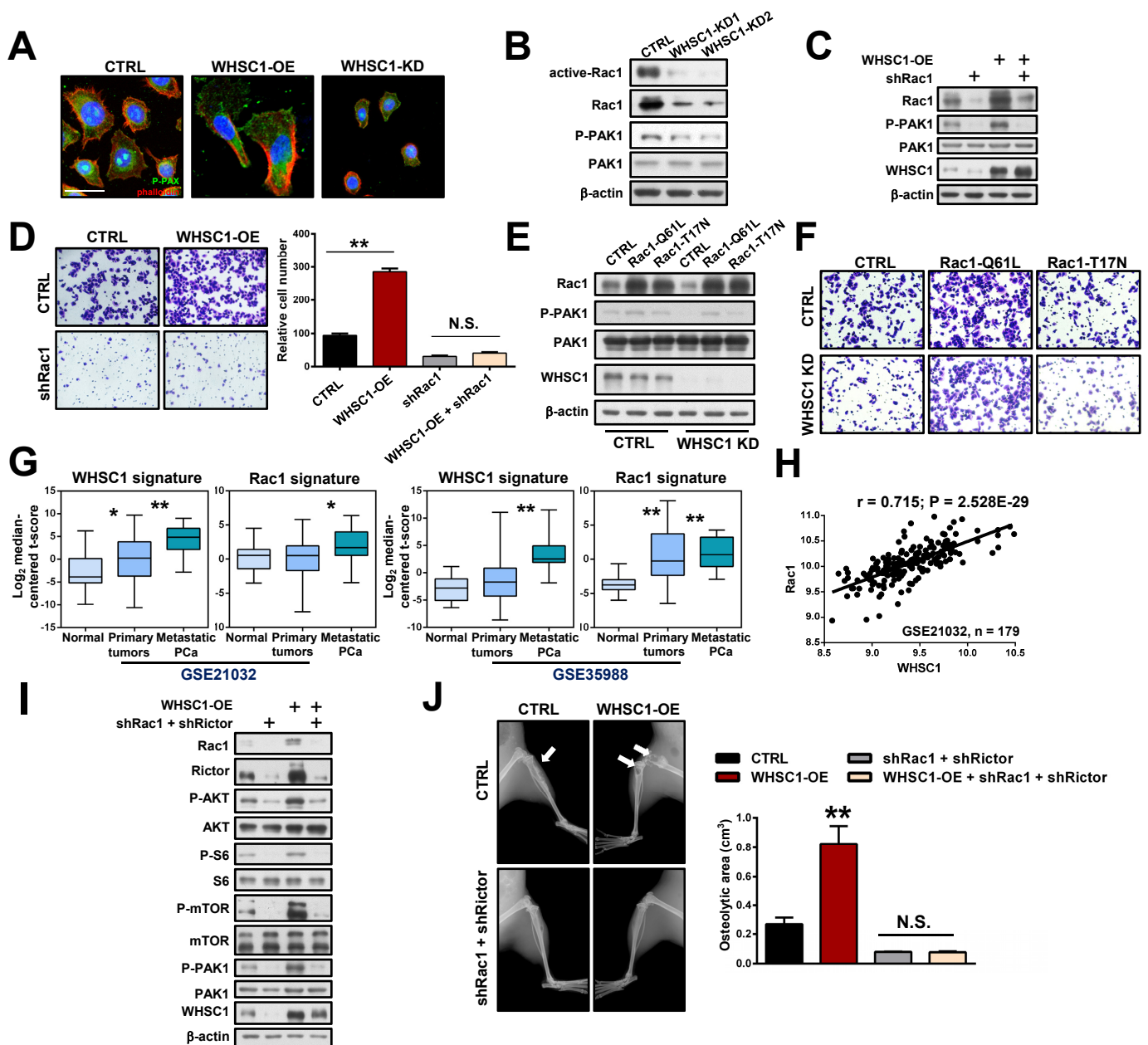


Supplemental Figure 6. Phosphorylation of WHSC1-S172 prevents the destruction mediated by CRL4^{Cdt2}. (A) IB analysis of 293T cells transfected with the indicated Scramble or CUL4B, CUL4A and Cdt2 shRNA. (B) Immunoblot analysis of WCL and immunoprecipitates derived from 293T cells transfected with Flag-WHSC1, or Flag-WHSC1-S172A, wild-type CUL4B or enzymatic dead CUL4B dominant negative (CUL4B-DN) and HA-Ub constructs. (C) Immunoblot analysis of WCL and immunoprecipitates derived from 293T cells transfected with Flag-CUL4B and the indicated HA-tagged wild type WHSC1, WHSC1-S172A or phosphor-mimic WHSC1-S172D construct.

Supplemental Figure 7



Supplemental Figure 8



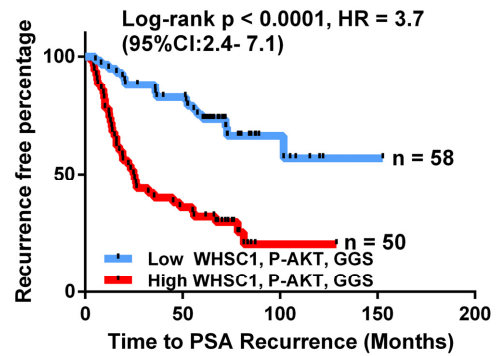
Supplemental Figure 8. WHSC1 regulates Rac1 expression to promote PCa tumorigenesis. (A) Phospho-Paxillin immunostaining in control, WHSC1-OE and WHSC1-KD PC3 cells. (B) Active Rac1, total Rac1, and their downstream effectors in cells. (C-D) Immunoblot analysis of WCL (C) and migration assay (n = 3) (D) in control and WHSC1 over-expressed PC3 with or without Rac1 knockdown. (E) Immunoblot analysis of WCL (E) and migration assay (F) in control and WHSC1 knockdown PC3 with or without constitutively active Rac1 (Rac1-Q61L) or dominant negative Rac1 (Rac1-T17N) over-expression. (G) WHSC1 signature (GSE84868) and Rac1 signature (GSE78093) in normal, primary versus metastatic PCa specimens from patients (using dataset: GSE21032, n = 179, and GSE35988, n = 88), in which each tumor expression profile was scored by t score for manifestation of the WHSC1 or Rac1 gene activity. p values are examined by two-sided One-way ANOVA. (H) The correlation between WHSC1 and Rac1 transcripts in patients is shown in regression plots (GSE21032, n = 179). Pearson correlation coefficients test is used to determine statistical significance. (I) IB analysis of WCL in control or WHSC1 overexpressed PC3 cells with or without Rictor and Rac1 depletion. (J) Representative X-ray images for bone metastasis are shown in left panel, and osteolytic area sizes are quantified in right panel. Results are presented as mean \pm SEM. **: $p < 0.01$. Arrow denotes areas of osteolysis (n = 8 per group). Scale bars: 10 μ m (A).

Supplemental Figure 9

A

Asian radical prostatectomy cohort, n = 108			
Multivariate Cox	P value	HR	95% CI
Gleason Score	0.014	1.63	1.10 to 2.41
PSA	0.030	1.92	1.07 to 3.46
WHSC1	0.001	2.54	1.46 to 4.42
P-AKT	0.005	2.19	1.27 to 3.79

B



Supplemental Figure 9. Prognostic potential of WHSC1 and AKT signaling in human Pca. (A) Multivariate Cox regression analysis of the levels of WHSC1, phospho-AKT, PSA levels and Gleason score at diagnosis of BCR in TMA (n = 108). **(B)** Kaplan–Meier plot (p-values by log-rank test) of patients grouped using the combination of WHSC1, phospho-AKT and Gleason score (K-means clustering) in TMA.

Supplemental Table 1. Summary of the clinical information of GSE21032, GSE40272, GSE6919 and GSE35988

Variables	GSE21032	GSE6919	GSE35988	GSE40272
Numbers	179	171	88	78
Normal sample	29	81	12	35
Primary tumors	131	65	49	43
Metastatic PCa	19	25	27	
Samples with clinical follow up, n	140			33
Age at diagnosis, yr.	37.3 - 83			44 - 73
No. of biochemical recurrence, n (%)	36 (25.7%)			9 (27.3%)
Preoperative PSA, ng/mL	12.1 (1.15 - 506)			
	≤6 78 (55.7%)			
Pathologic Gleason score, n	7 49 (35.0%)			
	≥8 13 (9.3%)			
Seminal vesicle invasion	20 (14.3%)			
Lymph node invasion	12 (8.6%)			

Supplemental Table 2. The clinical information of Asian radical prostate cohort

Variables	All patients
Numbers	128
Age at diagnosis, yr.	61 - 71
Year of surgery	2006 - 2010
No. of biochemical recurrence, n(%)	47 (39.8)
Preoperative PSA, ng/mL	16.0 (10.4-31.6)
Pathologic Gleason score, n (%)	
≤6	29 (24.6)
7	53 (44.9)
8	21 (17.8)
≥9	15 (12.7)
Adverse pathologic events, n (%)	
Seminal vesicle invasion	13 (11.0)
Lymph node invasion	4 (3.4)
Positive surgical margins	6 (5.1)

Supplemental Table 3. Univariate analysis of WHSC1, PTEN , Rac1 signature, mTOR signature and other parameters in BCR

Univariate cox	Group	Log-rank p value	HR	95% CI
WHSC1	Low	0.006	1.78	1.14 to 2.77
	Middle			
	High			
PTEN	Low	0.001	0.49	0.32 to 0.77
	Middle			
	High			
RAC1 signature	Low	0.012	1.88	1.22 to 2.89
	Middle			
	High			
mTOR signature	Low	0.206	1.54	0.79 to 3.00
	High			
PSA	(0,10)	p < 0.0001	2.36	1.43 to 3.89
	[10,20)			
	≥20			
Combined GGS	<7	p < 0.0001	2.80	1.80 to 4.36
	7			
	>7			
Taylor et al. GSE21032, n = 140				
Univariate cox	Group	Log-rank p value	HR	95% CI
WHSC1	Low	p < 0.0001	2.91	1.69 to 5.0
	High			
P-AKT	Low	p < 0.0001	2.77	1.62 to 4.73
	High			
PSA	(0,20)	p < 0.0001	2.87	1.68 to 4.9
	≥20			
Combined GGS	<7	0.001	1.95	1.36 to 2.81
	7			
	>7			

Asian radical prostate cohort TMA; n = 108

Supplemental Table 4. C-statistic analysis of TMA reveals that 2-gene set (WHSC1 and phospho-AKT) improves the prognostic accuracy of Gleason score and PSA

Models in TMA (BCR cases, n = 55; BCR-free cases, n = 53)

Model 1. Gleason only: C = 0.641 (95% CI = 0.565 - 0.716)

Model 2. PSA only: C = 0.622 (95% CI = 0.557 - 0.686)

Model 3. 2-genes (WHSC1, p-AKT) only: C = 0.674 (95% CI = 0.606 - 0.741)

Model 4. Gleason + 2-genes: C = 0.731 (95% CI = 0.652 - 0.811)

Model 5. PSA + 2-genes: C = 0.718 (95% CI = 0.642 - 0.793)

Supplemental Table 5. The shRNA , giRNA and siRNA sequences are listed.

giRNA	
WHSC1	CACCGATATGACTCCTTGCTGGAGC AAACGCTCCAGCAAGGAGTCATATC

shRNA	
shWHSC1-1	CCGGCCCTTCGCAGTGTTTGTCTTACTCGAGTAAGACAAACACTGCGAAGGGTTTTTG AATTCAAAAACCTTCGCAGTGTTTGTCTTACTCGAGTAAGACAAACACTGCGAAGGG
shWHSC1-2	CCGGTGCCAATAACACGTCCACTCTCGAGAGTGGACGTGTTATTGGCATTTTTTG AATTCAAAAATGCCAATAACACGTCCACTCTCGAGAGTGGACGTGTTATTGGCA
shRictor-1	CCGGCGTCGGAGTAACCAAAGATTACTCGAGTAATCTTTGGTTACTCCGACGTTTTTG AATTCAAAAACGTCCGAGTAACCAAAGATTACTCGAGTAATCTTTGGTTACTCCGACG
shRictor-2	CCGGCCGATCATGGGCAGGTATTATCTCGAGATAATACCTGCCCATGATCGGTTTTTG AATTCAAAAACCGATCATGGGCAGGTATTATCTCGAGATAATACCTGCCCATGATCGG
shRac1-1	CCGGCCCTACTGTCTTTGACAATTACTCGAGTAATTGTCAAAGACAGTAGGGTTTTTG AATTCAAAAACCTACTGTCTTTGACAATTACTCGAGTAATTGTCAAAGACAGTAGGG
shRac1-2	CCGGCCTTCTTAACATCACTGTCTTCTCGAGAAGACAGTGATGTTAAGAAGTTTTTG AATTCAAAAACCTTCTTAACATCACTGTCTTCTCGAGAAGACAGTGATGTTAAGAAGG
shCUL4A-1	CCGGGCCAAAGGTTAATGCAGGAAACTCGAGTTTCTGCATTAACCTTTGGCTTTTTG AATTCAAAAAGCCAAAGGTTAATGCAGGAAACTCGAGTTTCTGCATTAACCTTTGGC
shCUL4A-2	CCGGCCATGATATGTGGTCTAAGAACTCGAGTTCTTAGACCACATATCATGGTTTTTG AATTCAAAAACCATGATATGTGGTCTAAGAACTCGAGTTCTTAGACCACATATCATGG
shCUL4B-1	CCGGGCTGTCTGATTTGCAAATTTACTCGAGTAAATTTGCAAATCAGACAGCTTTTTG AATTCAAAAAGCTGTCTGATTTGCAAATTTACTCGAGTAAATTTGCAAATCAGACAGC
shCUL4B-2	CCGGGCAATTCTTCAGAAAGGTTTACTCGAGTAAACCTTTCTGAAGAATTGCTTTTTG AATTCAAAAAGCAATTCTTCAGAAAGGTTTACTCGAGTAAACCTTTCTGAAGAATTGC
shCdt2-1	CCGGCTGGTGAACCTAACTTGTTACTCGAGTAACAAGTTTAAGTTCACCAGTTTTTG AATTCAAAAACCTGGTGAACCTAACTTGTTACTCGAGTAACAAGTTTAAGTTCACCAG
shCdt2-2	CCGGCCTAGTAACAGTAACGAGTACTCGAGTACTCGTACTGTTACTAGGCTTTTTG AATTCAAAAAGCCTAGTAACAGTAACGAGTACTCGAGTACTCGTACTGTTACTAGGC

siRNA	
siCdt2-1	GAAUUUACUGCUUAUCGA
siCdt2-2	AAGGUUCCUGGUGAACUAAA
siCUL4B-1	GGUGAACACUUACAGCAA
siCUL4B-2	AAGCCUAAAUUACCAGAAA
siWHSC1-1	GCACACGAGAACGACAUCA
siWHSC1-2	UGUCAGUGGAGGAGCGGAA

Supplemental Table 6. The qRT-PCR and ChIP-qPCR primer sequences are listed.

qRT-PCR primer	
WHSC1	ACTCCGAGCTGCGAGGTGAAC
	AAGTAAGATCTTTCAGCTTGTCG
PTEN	TTGGCGGTGTCATAATGTCT
	GCAGAAAGACTTGAAGGCGTA
β-actin	AGAGCTACGAGCTGCCTGAC
	AGCACTGTGTTGGCGTACAG
ChIP-qPCR Primer	
Rictor-1	TGGTCCTTTATCATTCTTGCTC
	AAGGGAACCTCTTGAGTCCAGTC
Rictor-2	GAAGTATAAGAGTGGCTTGCTG
	TGTTGTTTCCTAAGTCTGCGTGT
Rictor-3	ACAGAGTTTCCCAATCTGCTTCA
	GCTAACAAATATCCATCTTCCCTAA
Rictor-4	ATGCCTACTCCTGCTTCACCTTC
	GTCCTCCAAACTCTTCCAACCTCT
Rictor-5	GCAGGTCCCAGATACCATCCTTA
	GTTCATAAAGGAGGTAACAAGACAA
Rac1-1	CCTGTATTCACCGCTACTCAACC
	TTTCCATCAACCTATTTCCACGT
Rac1-2	AGCGTTGCTTGATAGGTTAGTGT
	ATGCCAGAACTTTCCTTGGACTION
Rac1-3	GGTTGATTAAAGGAATGGGAACG
	TGTAAGGATGATGTCACGGAAGG
Rac1-4	TTATTGTTGAGATGGGATCGTGC
	AGTGGTGGCTCTTGCTGTAGTC
Rac1-5	GGTCATTTAACATTGGCATCCTC
	CGACTACCTGCTCACCATCTTTT
β-actin	GTGCTCAGGGCTTCTTGCTCTTCC
	TTTCTCCATGTCGTCCAGTTGGT